Counting and correcting thermodynamically infeasible flux cycles in genome-scale metabolic networks

An Adaptive Algorithm for Fully Automated Extraction of Passive Parameterized Macromodels

Elisa Fevola, Alessandro Zanco, Stefano Grivet-Talocia, Tommaso Bradde, Marco De Stefano
Dept. Electronics and Telecommunications, Politecnico di Torino, Torino, Italy
{elisa.fevola,alessandro.zanco,stefano.grivet,tommaso.bradde,marco.destefano}@polito.it

***Abstract*—We present a general framework for the fully automated extraction of stable and passive parameterized macromodels from sampled frequency responses. The proposed iterative algorithm provides an automated selection of the optimal parameter configurations to be simulated by a field solver, based on a combination of data-driven and model-driven metrics. The resulting frequency responses are fitted by a parameterized rational macromodel, whose uniform stability and passivity are enforced. We demonstrate the effectiveness of this framework on a transmission-line network test case.**

I. Introduction

Parameterized macromodels provide a common tool both in academia and in industry for fast simulation and optimization of electromagnetic structures [5]. Such reduced-order models provide an approximation of the response of a given structure in state-space form, where the response depends both on frequency and on a number of geometry or material parameters. Macromodels can be simulated in time or frequency domain, and their numerical simulation at the system level is usually orders of magnitude faster than a full-wave simulation of the underlying electromagnetic problem. Therefore, after a suitable identification process, the macromodel provides a surrogate that is able to replace the original structure in those optimization and sensitivity studies that are required during design flows.

Macromodel construction may require a large number of electromagnetic simulations, since enough information must be retrieved on the original system response for enabling an accurate approximation. Here, with simulation we intend a frequency sweep of the system (scattering) response for a given parameter configuration, usually based on a differential or integral equation frequency-domain solver. This problem becomes critical when the number of geometrical parameters increases. A brute-force tensor-product parameter sweep would lead to an exponential growth in the number of required simulations, which is of course impractical. Hence the need of determining the minimal number of field simulations that are strictly necessary for the extraction of an accurate macromodel.

The above scenario is further complicated by the essential requirements on the final parameterized macromodel to be stable and passive uniformly in the parameter space. If these requirements are not met, the macromodel will not be reliable in time-domain simulations since instabilities may occur [2], [5]. More in general, unstable and/or non-passive macromodels are physically inconsistent with the underlying system under modeling, provided that such system is a passive structure, device or component. This is indeed the main focus of this investigation.

The starting point of our work is [1], which presented an automated adaptive sampling process to determine the best candidate points in the parameter space that enable a reliable macromodel construction. The approach of [1] is purely *data-driven*, since only the characteristics of the original responses are used to set up the adaptive sampling scheme. Our approach is different, since also a set of *model-driven* criteria and metrics are used to support adaptive sampling. In particular, we tune the selection of the candidate simulation points based on the local model approximation error and on the results of a local passivity characterization. The latter is enabled by the recent developments documented in [3]. We show that the introduction of the latter two metrics enables macromodel construction with a significantly reduced number of simulations, and at the same time drives the iterative identification process towards a more accurate and uniformly passive and stable parameterized macromodel.

II. An Adaptive Algorithm for Point Selection

We denote as $\breve{\mathbf{H}}_{k,q} = \breve{\mathbf{H}}(\mathrm{j}2\pi f_k; \boldsymbol{\vartheta}_q)$ the response of the original system obtained from a field solver at frequency f_k with $k = 1, \ldots, \bar{k}$ and parameter configuration $\boldsymbol{\vartheta}_q$ with $q = 1, \ldots, \bar{q}$, where $\boldsymbol{\vartheta} = (\vartheta^1, ..., \vartheta^\rho)^\mathsf{T} \in \Theta \subset \mathbb{R}^\rho$ is a vector collecting the free geometry or material parameters of interest. The objective is here to determine a minimal number $\bar{q}$ and the optimal values of parameter configurations $\boldsymbol{\vartheta}_q$, so that a parameterized macromodel $\mathbf{H}(s; \boldsymbol{\vartheta})$ can be constructed, under the following constraints

1) the model vs data error is below a prescribed threshold
$$\|\mathbf{H}(\mathrm{j}2\pi f_k; \boldsymbol{\vartheta}_q) - \breve{\mathbf{H}}_{k,q}\| < \varepsilon \quad \forall k, q$$
2) the model is uniformly stable and passive, i.e., the following *Uniform Bounded Realness* conditions are satisfied
   a) $\mathbf{H}(s; \boldsymbol{\vartheta})$ regular for $\Re\{s\} > 0$, $\forall \boldsymbol{\vartheta} \in \Theta$,
   b) $\mathbf{H}^*(s; \boldsymbol{\vartheta}) = \mathbf{H}(s^*; \boldsymbol{\vartheta})$ $\forall s \in \mathbb{C}$, $\forall \boldsymbol{\vartheta} \in \Theta$,
   c) $\mathbf{I} - \mathbf{H}^\mathsf{H}(s; \boldsymbol{\vartheta})\mathbf{H}(s; \boldsymbol{\vartheta}) \geq 0$ for $\Re\{s\} > 0$, $\forall \boldsymbol{\vartheta} \in \Theta$.

The idea of employing an adaptive scheme for selecting simulation points is not new, as a good adaptive sampling algorithm was already presented in [1]. That approach was

based on two *exploration* and *exploitation* criteria, which were properly combined into a final metric for point selection. The scheme proposed here is similar, with the addition of two other model-driven criteria that embed in the point selection process appropriate metrics related to the actual final objective of reaching an accurate and passive model, and expressed by the two constraints 1) and 2) above.

The algorithm starts with a set of initial points, which correspond to a set of $\bar{q}_0$ system responses $\mathcal{Q}_0 = \{\boldsymbol{\vartheta}_1, \ldots, \boldsymbol{\vartheta}_{\bar{q}_0}\}$ scattered in the parameter space Θ. Each simulation point $\boldsymbol{\vartheta}_q = (\vartheta_q^1, ..., \vartheta_q^\rho)$ is associated to a specific combination of scalar values assumed by the parameters. At any subsequent ν-th iteration, with $\nu > 0$, a new set of points $\mathcal{P}_\nu$ is added to the already existing sets, so the total set of simulation points, composed of $\bar{q}_\nu$ elements, becomes $\mathcal{Q}_\nu = \mathcal{Q}_{\nu-1} \cup \mathcal{P}_\nu$. Figure 1 illustrates the adaptive addition of points (green dots) through iterations on a test case. At each iteration, the parameter space is partitioned into disjoint cells C_q^ν, with each cell associated to a single $\boldsymbol{\vartheta}_q$ with $q \in \mathcal{Q}_\nu$. The cells are defined through a Voronoi tessellation supported by the current point distribution, as in [1]. Then, the cells are ranked based on a metric that combines four independent criteria, which are itemized and discussed below. The cells with highest rank will host the new points $\boldsymbol{\vartheta}_q$ with $q \in \mathcal{P}_\nu$ to be added for the next iteration.

A. Exploration

The *exploration* criterion aims at positioning new points in such a way that the entire design space is explored [1]. Based on this criterion, new points will be added in those regions with a coarser sampling density. This can be achieved by ranking each cell C_q (iteration index ν is omitted from now on) based on its normalized volume $V(C_q)$. Therefore, we define as in [1] the exploration metric as

$$\Lambda_1(\boldsymbol{\vartheta}_q) = \frac{V(C_q)}{\sum_{q=1}^{q=\bar{q}} V(C_q)} \tag{1}$$

B. Exploitation

The *exploitation* criterion aims at placing new points in the regions where the system response undergoes a large variation, based on the assumption that rapid variations should require a finer sampling density. Also this criterion was already defined and used in [1] and is briefly summarized below.

The variation of the response at each point $\boldsymbol{\vartheta}_q$ is evaluated with respect to a set of $L = 2\rho$ properly selected neighbouring points $\mathcal{N}(\boldsymbol{\vartheta}_q) = \{\boldsymbol{\vartheta}_{q,\ell}\}_{\ell=1}^{L}$, which surround the central point in all directions. Exploitation is obtained in practice by calculating an approximation of the gradient $\nabla\breve{\mathbf{H}}(s_k;\boldsymbol{\vartheta})$ for each frequency s_k, which is used to compute the best local linear approximation $\bar{\mathbf{H}}(s_k;\boldsymbol{\vartheta}) \approx \breve{\mathbf{H}}(s_k;\boldsymbol{\vartheta})$ at any point $\boldsymbol{\vartheta}_q$. The distance between such local linear approximation and the true response $\breve{\mathbf{H}}(s_k;\boldsymbol{\vartheta})$ at the neighbouring points $\boldsymbol{\vartheta}_{q,\ell}$, after a proper normalization, constitutes the exploitation metric

$$\Lambda_2(\boldsymbol{\vartheta}_q) = \frac{E(\boldsymbol{\vartheta}_q)}{\sum_{q=1}^{\bar{q}} E(\boldsymbol{\vartheta}_q)} \tag{2}$$

where

$$E(\boldsymbol{\vartheta}_q) = \max_k \left(\sum_{\ell=1}^{L} \left\| \bar{\mathbf{H}}(s_k;\boldsymbol{\vartheta}_{q,\ell}) - \breve{\mathbf{H}}(s_k;\boldsymbol{\vartheta}_{q,\ell}) \right\| \right) \tag{3}$$

C. Data-model relative error

At each iteration, after a set of new additional points has been selected, an intermediate macromodel $\mathbf{H}(s;\boldsymbol{\vartheta})$ is generated. The main engine that we use here for macromodel construction is the Parameterized Sanathanan-Koerner (PSK) iteration, see e.g. [7], [8], which seeks for a model in form

$$\mathbf{H}(s;\boldsymbol{\vartheta}) = \frac{\mathbf{N}(s;\boldsymbol{\vartheta})}{\mathsf{D}(s;\boldsymbol{\vartheta})} = \frac{\sum_{n=0}^{\bar{n}} \sum_{\ell=1}^{\bar{\ell}} \mathbf{R}_{n,\ell}\, \xi_\ell(\boldsymbol{\vartheta})\, \varphi_n(s)}{\sum_{n=0}^{\bar{n}} \sum_{\ell=1}^{\bar{\ell}} r_{n,\ell}\, \xi_\ell(\boldsymbol{\vartheta})\, \varphi_n(s)} \tag{4}$$

where $\varphi_n(s)$ and $\xi_\ell(\boldsymbol{\vartheta})$ are frequency-domain and parameter-space basis functions and $\mathbf{R}_{n,\ell}$, $r_{n,\ell}$ are the model coefficients that are numerically found through an iterative process. An equivalent form of this model is the parameterized state-space (descriptor) form [7]

$$\mathbf{H}(s;\boldsymbol{\vartheta}) = \mathbf{C}(\boldsymbol{\vartheta})\,(s\mathbf{E} - \mathbf{A}(\boldsymbol{\vartheta}))^{-1}\,\mathbf{B} \tag{5}$$

with

$$\mathbf{A}(\boldsymbol{\vartheta}) = \sum_{\ell=1}^{\bar{\ell}} \mathbf{A}_\ell\, \xi_\ell(\boldsymbol{\vartheta}), \quad \mathbf{C}(\boldsymbol{\vartheta}) = \sum_{\ell=1}^{\bar{\ell}} \mathbf{C}_\ell\, \xi_\ell(\boldsymbol{\vartheta}). \tag{6}$$

The relative error between such model and original data at each simulation point is used as a third metric for point selection, based on the assumption that more samples are needed where the current model is not accurate enough. Note that an automated model order estimation is embedded in our implementation of the PSK iteration, so that model accuracy is maximized automatically by choosing the proper model orders. Therefore, an inaccurate intermediate model is likely due to an insufficient sampling density. The error-based metric is thus expressed as

$$R^2(\boldsymbol{\vartheta}_q) = \frac{\sum_k ||\mathbf{H}(s_k;\boldsymbol{\vartheta}_q) - \widetilde{\mathbf{H}}(s_k;\boldsymbol{\vartheta}_q)||^2}{\sum_k ||\breve{\mathbf{H}}(s_k;\boldsymbol{\vartheta}_q)||^2} \tag{7}$$

and then properly normalized as

$$\Lambda_3(\boldsymbol{\vartheta}_q) = \frac{R(\boldsymbol{\vartheta}_q)}{\sum_{q=1}^{\bar{q}} R(\boldsymbol{\vartheta}_q)}. \tag{8}$$

D. Passivity violations

The final target of the presented approach is an accurate, stable and passive macromodel. Even assuming that data retrieved from a field solver are passive, the inevitable approximations of the fitting process can lead to a non-passive model at any stage of proposed iterative model construction. Although passivity on the model must always be checked and (if needed) enforced, the selection of new simulation points can be driven by sampling more densely the regions of the parameter space where the intermediate model is not passive. This is achieved by means of a dedicated metric, which measures the extent of model passivity violations.

Considering condition 3) of Sec. II, we see that the model is passive at any point $(s, \boldsymbol{\vartheta})$ when the maximum singular value of the model response does not exceed one, $\sigma_{\max}(\mathbf{H}(s;\boldsymbol{\vartheta})) \leq 1$. Therefore, the extent of a local passivity violation can be measured in terms of the maximum singular value as

$$S(\boldsymbol{\vartheta}_q) = \max_{\omega \in \mathbb{R}} \ \sigma_{\max}(\mathbf{H}(s;\boldsymbol{\vartheta}_q)) \tag{9}$$

This maximum is obtained by launching a Hamiltonian passivity check on the model instantiated at $\boldsymbol{\vartheta}_q$, using the procedure of [2], [3]. The Skew-Hamiltonian/Hamiltonian (SHH) matrix pencil $(\mathbf{M}_S(\boldsymbol{\vartheta}_q), \mathbf{K}_S)$ defined as

$$\mathbf{M}_S(\boldsymbol{\vartheta}_q) = \begin{pmatrix} \mathbf{A}(\boldsymbol{\vartheta}_q) & \mathbf{B}\mathbf{B}^\mathsf{T} \\ -\mathbf{C}^\mathsf{T}(\boldsymbol{\vartheta}_q)\mathbf{C}(\boldsymbol{\vartheta}_q) & -\mathbf{A}^\mathsf{T}(\boldsymbol{\vartheta}_q) \end{pmatrix} \tag{10}$$

$$\mathbf{K}_S = \begin{pmatrix} \mathbf{E}^\mathsf{T} & \mathbf{0} \\ \mathbf{0} & \mathbf{E} \end{pmatrix}$$

is constructed, and its eigenvalues are computed. The frequency bands $(\omega_i(\boldsymbol{\vartheta}_q), \omega_{i+1}(\boldsymbol{\vartheta}_q))$ where local passivity violations are present are obtained by postprocessing this eigenspectrum. Combination of this test with a Hamiltonian eigenvalue perturbation process at each $\boldsymbol{\vartheta}_q$ leads to a precise tracking of the boundaries that separate the regions in Θ where the model is passive/non-passive. Such regions are depicted with green and red dots, respectively, in Fig. 3, see also [3]. The maximum singular value required in (9) is easily obtained by a local fine sampling in each detected non-passive band of the local model $\mathbf{H}(s;\boldsymbol{\vartheta}_q)$.

As a result, the cells C_q are ranked based on the normalized passivity violations as

$$\Lambda_4(\boldsymbol{\vartheta}_q) = \frac{S(\boldsymbol{\vartheta}_q)}{\sum_{q=1}^{\bar{q}} S(\boldsymbol{\vartheta}_q)}. \tag{11}$$

E. Adaptive selection of new points

The four metrics Λ_i, $i = 1, \ldots, 4$ are combined into a single global metric

$$\Lambda(\boldsymbol{\vartheta}_q) = \prod_{i=1}^{4} [1 + \alpha_i \Lambda_i(\boldsymbol{\vartheta}_q)] \tag{12}$$

where the coefficients $\alpha_i > 0$ can be further used to tune the importance of each individual criterion. This global metric is used to rank data points and their associated Voronoi cells: the new points will be finally placed inside the Voronoi cells with higher ranking, as in [1]. As already mentioned, the algorithm works iteratively, so the addition of new points is repeated until a sufficiently accurate model is obtained. At each iteration ν, a fraction of $\beta = |\mathcal{P}_\nu|/|\mathcal{Q}_{\nu-1}|$ samples are added, where $0 < \beta < 1$. We have observed that $\beta = 1/3$ provides a good trade-off between number of added points at each iteration and number of required iterations.

III. Passivity Enforcement

After a sufficient number of simulation points has been selected and an accurate model has been obtained, its passivity (and thus also its stability) is checked and, if necessary, enforced. The procedures used both for stability/passivity check and enforcement are those presented in [2], [3], [6], which the Reader is referred to for further details.

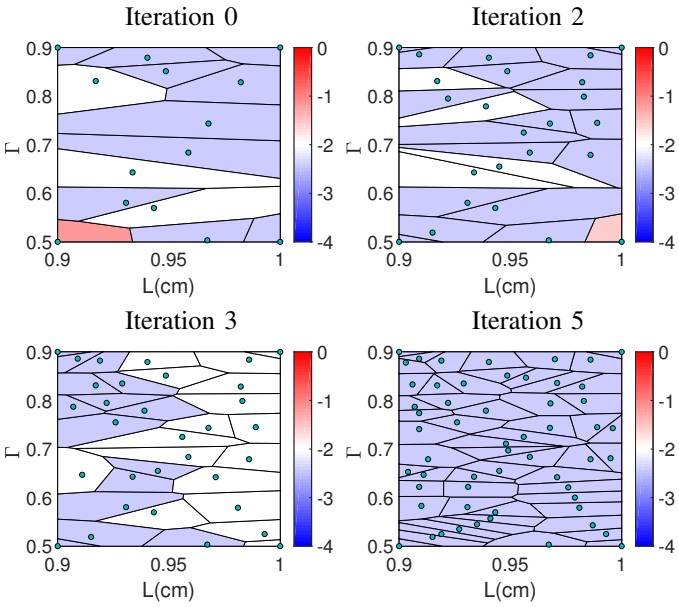

Fig. 1: Voronoi diagram of the parameter space at different iterations for the distributed network example. The scale used to color each cell represents the model-data error at the corresponding sample point.

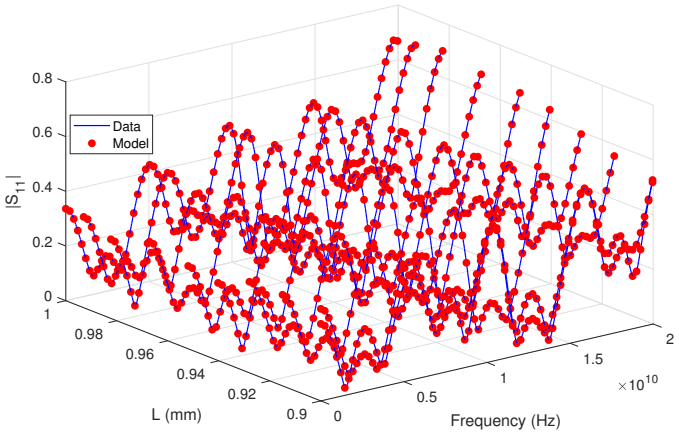

Fig. 2: Comparison between passive model and original data of the distributed network for a selected set of responses.

IV. Examples

We illustrate the effectiveness of our adaptive macromodeling framework on a distributed network. The structure is composed of four cascaded segments of a lossy transmission line, with three internal loaded stubs. In this case we parameterize the internal line lengths, here denoted as $\vartheta^1 = L \in [9, 10]$ mm, and the load terminating the central stub by means of its reflection coefficient $\vartheta^2 = \Gamma \in [0.5, 0.9]$. The remaining lengths are set to a fixed value of 7 mm, the stubs to 1 mm, while the reflection coefficients of the non parameterized loads are set to 0.5. We seek for a lumped

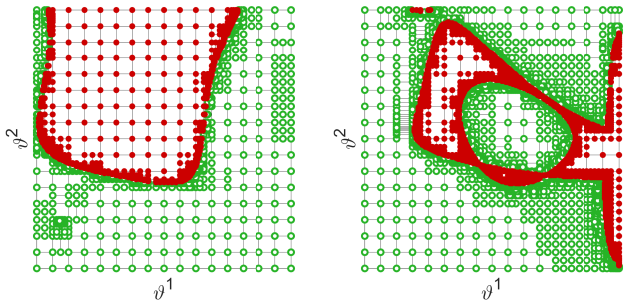

Fig. 3: Passivity check on the distributed network models costructed by driving adaptive sampling with (left) and without the passivity violation metric (right). Each green (red) dot denotes a parameter configuration for which the parameterized model is passive (non-passive).

(rational) parameterized macromodel of this structure, based on the adaptively determined frequency responses selected by proposed scheme. The frequency responses are obtained by a field solver.

The proposed adaptive sampling process terminates in 5 iterations, with a total of $\bar{q}_5 = 56$ simulation points in the two-dimensional parameter space. Figure 1 depicts the Voronoi tessellation of the design space at four selected iterations. Each cell is colored with a color scale that corresponds to the relative error (metric Λ_3) of the intermediate macromodel built with the current set of points. Note that the global metric is used to refine the grid, although only model error is displayed in the four figure panels. As Fig. 1 shows, the few red cells present at the first iterations, corresponding to regions where the model is still not enough accurate, progressively turn to blue, up to the final iteration where the model is uniformly accurate all over the space.

After the last iteration, passivity and stability of the model must be checked and, if necessary, enforced. In this case the model turns out to be already stable, but not passive. Therefore, we apply the parameterized passivity enforcement scheme of [3] to remove the residual passivity violations while preserving model accuracy. A comparison between data and final (passive) model responses is reported in Fig. 2, where the uniform model accuracy is confirmed.

In order to test the effectiveness of the passivity metric, which is one of the main novel aspects of this paper, the procedure has been repeated without including Λ_4 in the global metric (12). In this case the final model results unstable, so that also a postprocessing stability enforcement is necessary before enforcing passivity. All details of this process are reported in [3]. It turns out that the resulting model is not acceptable due to the excessive perturbation that is required to compensate for both stability and passivity violations. A comparison of the passivity checks on the final models (before enforcing passivity) is reported in Fig. 3.

We conclude this example by noting that applying the adaptive sampling method of [1], i.e., removing the model-based metrics Λ_3 and Λ_4 requires a total of $\bar{q} = 74$ points in order to reach the same model accuracy (here verified a posteriori, since not embedded in the identification loop), with a 25% saving. Running the proposed algorithm on several other test cases (not reported here) led to savings up to 80% in the number of required samples. Moreover, considering the cumulative runtime required to obtain the final passive model by means of the proposed adaptive algorithm, approximately 3% of the overall time is used for the point selection process of the algorithm, while the remaining 97% is due to the field solver. Therefore, we see that the introduction of the proposed model-driven metrics provides better models with reduced computational effort and runtime.

V. Conclusions

We presented a fully automated algorithm for the generation of stable and passive parameterized macromodels. The proposed approach is able to select, based on the combination of four different metrics, a quasi-minimal set of simulation points in the parameter space which lead to a uniformly accurate model through an identification process based on the Parameterized Sanathanan-Koerner iteration. Each of these points corresponds to a combination of the parameters that instantiates a well-defined geometry, whose frequency responses are determined on-demand by calling an external field solver. New points are iteratively added until the model results uniformly accurate throughout the parameter space. Stability and passivity of the model at intermediate iterations are used to drive the adaptive sampling process, and are enforced a-posteriori on the final model using a perturbation approach. The effectiveness of the proposed framework is illustrated on a distributed network test case.

References

[1] D. Deschrijver, K. Crombecq, H. M. Nguyen, and T. Dhaene, "Adaptive algorithm for macromodeling of parameterized S-Parameter Responses," IEEE Transactions on Microwave Theory and Techniques, vol. 59, no.1, pp. 39–45, 2011.

[2] S. Grivet-Talocia, "Passivity enforcement via perturbation of hamiltonian matrices," IEEE Transactions on Circuits and Systems I: Regular Papers, vol. 51, no. 9, pp. 1755–1769, 2004.

[3] A. Zanco, S. Grivet-Talocia, T. Bradde, and M. De Stefano, "Enforcing passivity of parameterized LTI macromodels via Hamiltonian-driven multivariate adaptive sampling," IEEE Transactions on Computer-Aided Design of Integrated Circuits and Systems, 2018.

[4] S. Boyd, V. Balakrishnan, and P. Kabamba. A bisection method for computing the H_∞ norm of a transfer matrix and related problems. *Mathematics of Control, Signals and Systems*, 2(3):207–219, 1989.

[5] S. Grivet-Talocia and B. Gustavsen, *Passive macromodeling: Theory and applications*. John Wiley & Sons, 2015, vol. 239.

[6] Grivet-Talocia, Stefano, "A perturbation scheme for passivity verification and enforcement of parameterized macromodels," *IEEE Transactions on Components, Packaging and Manufacturing Technology*, vol. 7, no. 11, pp. 1869–1881, 2017.

[7] P. Triverio, S. Grivet-Talocia, and M. S. Nakhla. A parameterized macromodeling strategy with uniform stability test. *IEEE Trans. Advanced Packaging*, 32(1):205–215, Feb 2009.

[8] C. Sanathanan and J. Koerner. Transfer function synthesis as a ratio of two complex polynomials. *Automatic Control, IEEE Transactions on*, 8(1):56–58, jan 1963.